# Strain Range Approximation for Estimating Fatigue Life of Lead-free Solder Interconnects Under Temperature Cycle Loading

**Michael Osterman**
**Center for Advanced Life Cycle Engineering (CALCE)**
**University of Maryland, College Park 20742**
**osterman@calce.umd.edu**

## Abstract

The ability to estimate the fatigue life of solder interconnects under life-cycle loading conditions is critical for ensuring the reliability of electronic hardware. While multiple models have been published and successfully demonstrated to estimate the fatigue life of solder interconnects, a strain range model based on the work of Engelmaier remains one of the most widely used. In estimating the strain range, Engelmaier developed separate formulations for leaded and leadless component package types. This paper provides a review of the model proposed by Engelmaier and model constants for the lead-free (tin silver copper) solder alloy. The model is applied to simulate a physical test and comparisons between the simulation and physical test results are provided. Results show a good correlation for leadless component package types for both the lead-free and lead based solder alloys. However, the comparison indicates the strain range approximation for leaded component types may be incorrect.

## Introduction

The transition to lead-free solder has renewed interest in methods for modeling the life expectancy of solder interconnects in electronic hardware. The ability to model fatigue life is important for estimating field reliability and for determining the acceleration of failure that occurs under controlled tests. For lead-based solder, several phenomenological solder joint fatigue models have been published and successfully demonstrated [1-5].

For most solder fatigue models, life is related to a selected stress metric in the form of a power law. For temperature-cycle-induced fatigue, cyclic strain range and cyclic strain energy are often used. For instance, CALCE has successfully used a cyclic strain energy modeling approach through which the strain energy is partitioned into elastic, creep, and plastic components in detailed finite element modeling [2]. Other researchers [3, 4, 5] have used the total inelastic strain energy or other strain energies as the basis for fatigue models.

In general, the cyclic strain energy models are used in conjunction with a detailed finite element analysis. However, analytic models have been derived by Engelmaier [1], Jih and Pao [6], and Clech [7]. With all these models, it should be recognized that the fatigue constants are highly dependent on the assumed material properties used in their derivation. As such, users should not mix fatigue model constants and material

constitutive models. Furthermore, fatigue models may not always be independent of package type. In all cases, caution should be used when applying any fatigue model.

As mentioned, one of the most widely referenced and used models is based on the work of Werner Engelmaier [1]. Engelmaier proposed a fairly simple model based on strain range, with fatigue life being estimated using a Coffin-Manson fatigue model. This formulation was adopted by the IPC and put forth in IPC-STD-785 [8]and later in IPC 9701 [9]. This paper provides a review of the simulation model proposed by Engelmaier and model constants derived from experimental test data. Finally, the strain range model is used to assess the life expectancy of hardware under test, and results of the assessment are compared with actual test results.

**Simulation Model**

Although many models are available [1-5], the strain range model proposed by Engelmaier is widely used due to the ease of calculation of its constants. The model is based on the low-cycle fatigue part of the more general Coffin-Manson equation. That fatigue life relationship is given by

$$N_f = \frac{1}{2}\left(\frac{\Delta\gamma}{2\varepsilon_f}\right)^{\frac{1}{c}} \tag{1}$$

where $N_f$ is the number of cycles to fifty percent failure, $\Delta\gamma$ is the cyclic strain range, $\varepsilon_f$ is the fatigue ductility constant for the solder material, and $c$ is the fatigue ductility exponent. For tin-lead eutectic solder under a temperature-cycle loading condition, the fatigue exponent is defined as

$$c = c_o + c_1 T_{sj} + c_2 \ln\left(1 + \frac{360}{t_{dwell}}\right) \tag{2}$$

where $T_{sj}$ is the medium cyclic temperature and $t_{dwell}$ is the dwell time at the maximum temperature.

For leadless packages, the strain range is approximated as

$$\Delta\gamma = F\left(\frac{L_d(\alpha_c - \alpha_s)\Delta T}{h}\right) \tag{3}$$

where $L_d$ is the distance to the neutral point over which the expansion due to thermal cycling occurs; $\alpha_c$ and $\alpha_s$ are the coefficients of thermal expansion of the component and the substrate, respectively; $\Delta T$ is the temperature range of thermal cycling ($T_{max} - T_{min}$); $h$ is the effective height of the solder joint; and $F$ is a model calibration constant.

For leaded packages, the strain range is approximated as

$$\Delta\gamma = \frac{FK_d(L_d\Delta\alpha\Delta T)^2}{(200\,psi\,Ah)} \tag{4}$$

where $K_d$ is the diagonal flexural lead stiffness and A is the effective solder bond area.

In reviewing the strain range approximations, the use of the square term for the temperature range appears to be questionable. In this form, it appears that an energy rather than a strain range formulation has been used. This issue will be revisited later in this paper.

**Lead-free Model Constants**

In the original reference [1], Engelmaier provided constants for the eutectic tin-lead solder used as the *de facto* industry standard. With the transition to lead-free solder, researchers have been conducting extensive tests to examine the suitability of various lead-free solders. Early in this process, the ternary tin-silver-copper solder alloy gained popularity due to its cost and performance. However, insufficient testing was being conducted to derive the model constants for the Coffin-Manson fatigue life relationship used by Engelmaier. To this end, CALCE conducted a multiple year test program designed to evaluate the impact of dwell time and mean temperature on lead-free solders and provide data for deriving the model constants for the fatigue ductility exponent [8]. In the CALCE study, ceramic leadless chip carriers (CLCC) components were used.

Using the data from the CALCE tests, the fatigue ductility exponent model constants for the tin-silver-copper solder alloy were derived [8], based on the statistically determined fifty-percent failure values. The values for eutectic tin-lead (SnPb) and Sn3.9Ag0.7Cu (SAC) are presented in Table 1.

**Table 1. Fitted Model Parameters**

| Solder Parameters | SnPb | SAC |
|---|---|---|
| $C_0$ | -0.502 | -0.347 |
| $C_1$ | -7.34E-04 | -1.74E-03 |
| $C_2$ | 1.45E-02 | 7.83E-03 |
| $\varepsilon_f$ | 2.25 | 3.47 |

For the solder ductility constant, $\varepsilon_f$,, the value was not adjusted for solder joint height or model calibration factor. In the CALCE tests, the model constants for eutectic tin-lead were found to be slightly different than the values presented by Engelmaier. However, the Engelmaier constants were found to fall within the ninety-percent confidence intervals provided by the regression fit. These model constants are used in the CALCE first-order thermal fatigue model based on Engelmaier's proposed models [1, 8 and 9].

A plot of fatigue curves generated by the fitted model constants, along with test data, is provided in Figure 1. The curves represent the estimated neutral distance versus cycles-to-failure for a cyclic temperatures range of 100°C with 15-minute and 75-minute dwells, respectively. From this graph, it can be observed that the slope of the fatigue curve for the lead-free solders is slightly shallower than that of the tin-lead solder. As a result, the models indicate that a condition will arise under which the lead-free solders will have less

durability than the tin-lead solder. As depicted below, a crossover occurs at the higher strain levels, represented as a higher $L_d$ or diagonal length.

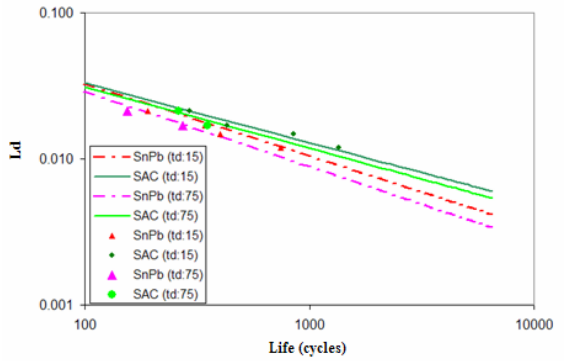


**Figure 1. Plot of the Derived Strain Range -based Solder Fatigue Models**

## Assembly Tests

As mentioned previously, the model constants presented by CALCE for the SAC solder were obtained by considering failure data on CLCC packages. This raises a concern that the model may be package-dependent. To explore this issue, the model was applied to temperature cycle test data reported under the lead-free solder study sponsored by the Joint Group for Pollution Prevention (JGPP) and the Joint Council for Aging Aircraft (JCAA) [11, 12]. In the JGPP/JCAA study, a board design was used that included a variety of conventional surface mount component package types. Package types included plastic ball grid array (PBGA), ceramic leadless chip carrier (CLCC), thin small outline package (TSOP), leadless resistors, and thin quad flat package (TQFP). Design assemblies were manufactured with lead-free (SAC) and lead-based solder and parts.

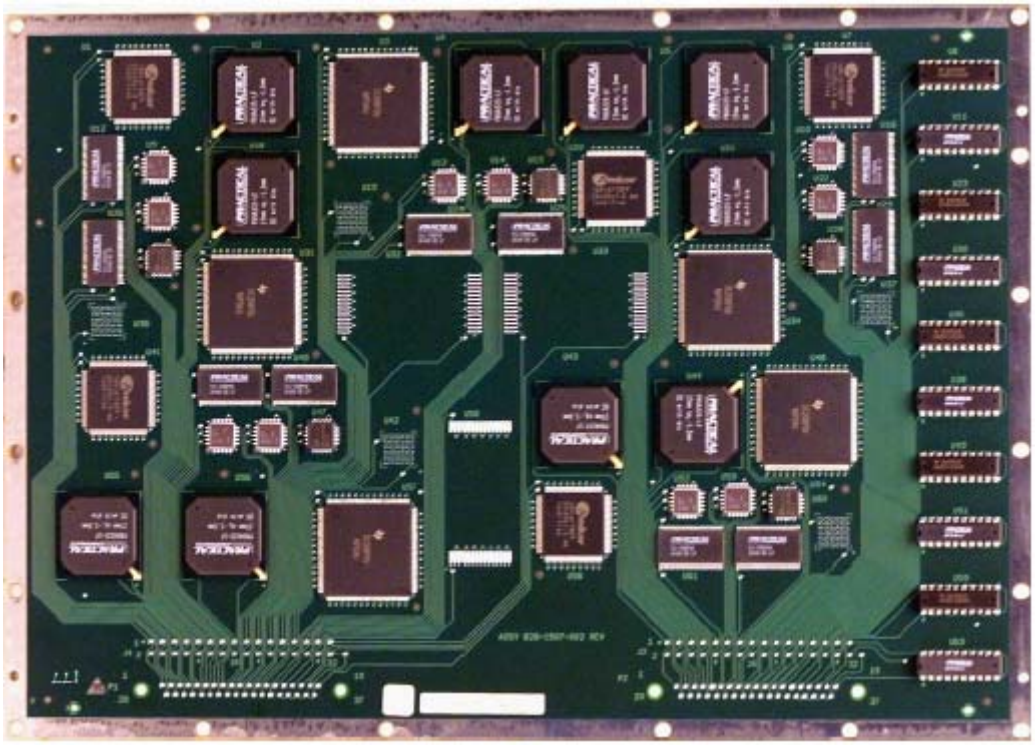

**Figure 2. JGPP/JCAA Test Assembly**

A photo of a test assembly for the JGPP/JCAA Lead-Free Solder Project is provided in Figure 2. In the JGPP/JCAA Lead-Free Solder Project, test assemblies were subjected to a variety of environmental loading conditions in an effort to compare the reliability of the lead-free assemblies with the conventional lead-based assemblies. For the purpose of this paper, we will focus on the temperature cycle test results from the JGPP/JCAA Lead-Free Solder Project.

In that study, two temperature-cycling conditions were applied to independent groups of test assemblies. The first test, conducted by Rockwell-Collins [11], subjected a set of test assemblies to a temperature cycle of -55 to 125$^{o}$C. The second test, conducted by Boeing [12], subjected another set of test specimens to a smaller temperature cycle of -20 to 80$^{o}$C. For both tests, the dwell time at the maximum temperature was 30 minutes and dwell time at the minimum temperature was 10 minutes.

To examine the accuracy of the derived tin-lead and SAC solder fatigue model constants, the JGPP/JCAA test assembly was modeled using the calcePWA software [10]. This software provides the ability to model a complete printed wiring board assembly and conduct temperature, vibration, and life assessments on the modeled design. The software includes a solder fatigue model based on the Engelmaier strain range approximations and the Coffin-Manson fatigue life relationship.

The calcePWA design model was based on design information derived from JGPP/JCAA reports and communication with study participants. The board model included six metallization layers and FR4 construction with an overall thickness of 2.34 mm. The

overall planar dimensions of the board were 323.8 mm by 228.6 mm. Part models were developed using calcePWA part model templates based on the specific package types. The part model templates parameterize part information in terms of geometric dimensions, including package length, package width, package thickness, interconnect span, and interconnect pitch. For leaded packages, the lead geometry is further parameterized. Package and lead materials are specified by reference to materials in an accompanying database. The material database provided with calcePWA includes definitions for material commonly used in construction of parts and printed wiring boards.

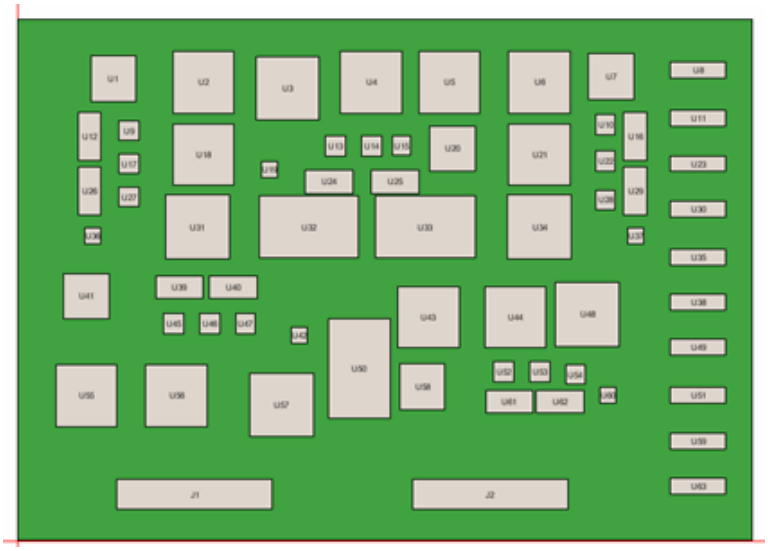

**Figure 3 calcePWA model of JGPP/JCAA board**

The part package geometry and material information was derived from manufacturer part datasheets, reports provided for the JGPP/JCAA study, and assumptions based on past modeling experience. The board position of each part on the JGPP/JCAA printed wiring board was estimated by measurements taken from design drawings. Assembly information, including solder bond area, solder joint height, and part standoff, were assumed based on past modeling experience. An image of the calcePWA design for the JGPP/JCAA assembly is presented in Figure 3. To simulate the tin-lead design, the CALCE tin-lead solder model, discussed previously, was selected. To simulate the lead-free version of the JGPP/JCAA design model, the solder material was changed to use the CALCE SAC solder model, which uses the Coffin-Manson fatigue life model constants presented earlier.

To simulate the temperature cycle test conditions used in the JGPP/JCAA study, two life profiles were developed in the calcePWA. The first profile, TC1, represents the -55 to 125$^{o}$C test condition; the second profile, TC2, represents the -20 to 80$^{o}$C temperature cycle. The calcePWA first-order thermal fatigue model effectively implements the strain range approximations and the Coffin-Manson fatigue life relationship proposed by Engelmaier [1, 8, and 9]. The primary variation in the CALCE first-order thermal fatigue model is that it includes internal calibrations for different package types based on accumulated test data and experience.

A comparison between the test results and the simulation results is provided in the following section.

**Results and Discussion**

The test results presented in both [11] and [12] included two-parameter Weibull plots, along with the evaluated characteristic life, $\eta$, and the shape parameter, β, for the distributions. The characteristic life for a Weibull distribution represents the time to 63.2 % percent failure of the samples ($N_{63.2\,\%}$). For the calcePWA first-order thermal fatigue model, the simulation results are calibrated for fifty percent failure. For comparison purposes, the number of cycles to fifty percent failure ($N_{50\,\%}$) was estimated for the JGPP/JCAA data from the reported Weibull parameters. Table 2 below lists the comparison between the simulated $N_{50\%,}$ based on the CALCE first-order thermal fatigue model and the $N_{50\%}$ calculated from the observed failure distribution of the components during accelerated testing. The results are graphically presented in Figure 4.

**Table 1. $N_{50\,\%}$ between reported and simulated values for various packages**

| | | | Data from [11, 12] | | | | |
|---|---|---|---|---|---|---|---|
| | Solder Material | Package type | $N_{63.2\,\%}$ (cycles) | β | $N_{50\,\%}$ (cycles) | $N_{50\,\%}$ (simulated) | Difference (%) |
| TC 1 | SnPb | CLCC20 | 709 | 5.7 | 664 | 473 | - 28.8 |
| | | PBGA225 | 2671 | 6.2 | 2516 | 1907 | - 24.2 |
| | | TQFP144 | 2672 | 7.4 | 2542 | 1834 | - 27.8 |
| | | PQFP208 | 3798 | 4.6 | 3506 | 3118 | - 11.1 |
| | | TSOP50 | 1180 | 7.6 | 1124 | 708 | - 37.0 |
| | SAC | CLCC20 | 508 | 6.54 | 480 | 435 | - 9.4 |
| | | PBGA225 | 3447 | 2.65 | 3002 | 2528 | -15.8 |
| | | TQFP144 | 3550 | 1.44 | 2754 | 2418 | -12.2 |
| | | PQFP208 | 8121 | 1.52 | 6381 | 5476 | -14.2 |
| | | TSOP50 | 1060 | 4.55 | 978 | 919 | - 6.0 |
| TC 2 | SnPb | CLCC20 | 1671 | 8.5 | 1600 | 1731 | 8.2 |
| | | PBGA225 | 7447 | 9.5 | 7164 | 7154 | - 0.1 |
| | | TQFP144 | 8670 | 7.3 | 8245 | 20282 | 145.9 |
| | | PQFP208 | NF[1] | NF | NF | 3377833778 | NF |
| | | TSOP50 | 3150 | 8.4 | 3016 | 7909 | 162.2 |
| | SAC | CLCC20 | 2360 | 5.7 | 2213 | 2599 | 17.4 |
| | | PBGA225 | NF | NF | NF | 16590 | NF |
| | | TQFP144 | 13175 | 8.6 | 12626 | 59486 | 371.1 |
| | | PQFP208 | NF | NF | NF | 11156 | NF |
| | | TSOP50 | 4148 | 6.7 | 3927 | 14354 | 265.5 |

[1] NF – Not sufficient number of failures to obtain a failure distribution

In Figure 4, the fifty percent lower bound and the one hundred percent upper bound line are also presented. For fatigue failure, a certain amount of scatter in the failure results is expected. However, the appropriateness of the model should be questioned where large variations are observed. The plotted upper and lower bounds represent expected variations with the current model. From this comparison, the simulation of the leadless and ball grid array packages shows good correlation with the test results. However, a significant variation is observed between simulation and test for the leaded TSOP and TQFP parts. Interestingly, this variation occurs for both the lead-free (SAC) and tin-lead solder.

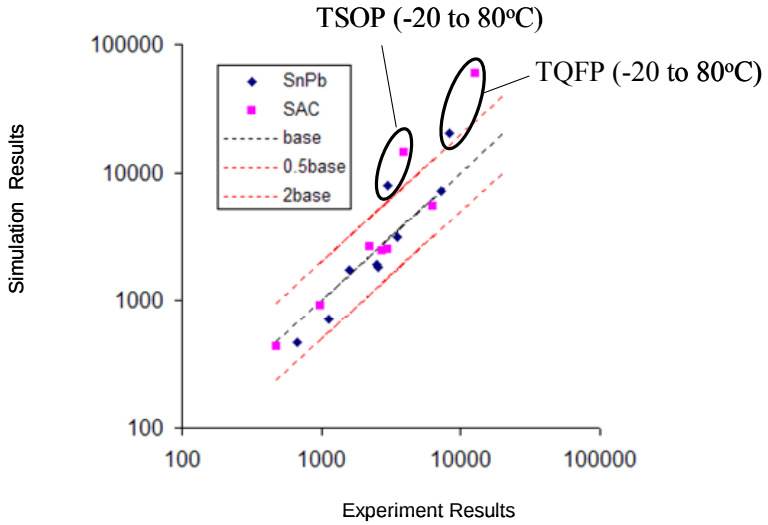


**Figure 4. Comparison of calcePWA results with experimental data [11,12].**

As touched on earlier, the strain range formulation proposed by Engelmaier differs significantly between leaded and leadless package types. In reviewing the formulation, the square term in the temperature range term is suspected as the primary driver for the overly optimistic estimate produced by the simulation model for the leaded parts. To verify this hypothesis, the TSOP and TQFP parts were modeled as leadless package types and the model calibration factors were adjusted to make the simulation results match closely with the test results for the TC1 condition. With the model calibration factors fixed, the simulation of the TC2 condition was made. The results for the leadless assumption for the TSOP and TQFP component are presented numerically in Table 2 and graphically in Figure 5.

**Table 2. TSOP and TQFP models as leadless packages**

| Part | Solder Alloy | TC1 | | | TC2 | | |
|---|---|---|---|---|---|---|---|
| | | CALCE Nf(50%) | TEST Nf(50%) | | CALCE Nf(50%) | TEST Nf(50%) | |
| **TSOP50** | SnPb | 1160 | 1124 | 3.19 | 4315 | 3016 | 43.06 |
| **TQFP144** | SnPb | 1861 | 2542 | -26.80 | 6980 | 8245 | -15.35 |
| | | | | | | | |
| **TQFP144** | SAC | 2467 | 2754 | -10.42 | 16099 | 12626 | 27.51 |
| **TSOP50** | SAC | 784 | 978 | -19.83 | 4827 | 3927 | 22.92 |

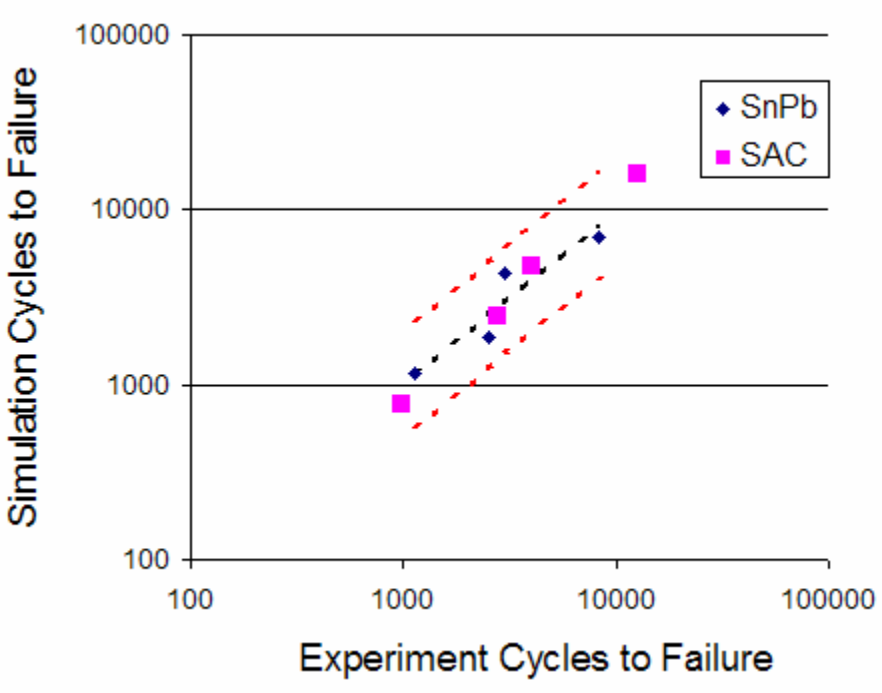


**Figure 5. TSOP and TQFP modeled as leadless packages**

From Figure 5 and Table 2, it can be observed that the leadless model matches the experimental results very well. This result strongly indicates that the formulation of the strain range value for the leaded parts is not appropriate for either tin-lead or lead-free (SAC) solders.

## Conclusions

The Coffin-Manson fatigue life relationship and the formulation of strain range based on the original work of Engelmaier has been presented. Model constants were provided for the Coffin-Manson fatigue relationship for tin-lead and tin-silver-copper solder alloys derived from experimental tests [10]. Comparison of physical test results with simulation results shows good correlation for leadless and plastic ball grid array parts. However, the strain range formulation for the leaded parts (TSOP and TQFP) resulted in a large, non-conservative estimate for fatigue life that did not match test results for either tin-lead or tin-silver-copper solders. Modeling the TSOP and TQFP parts using the leadless strain range approximation resulted in good correlation between test and simulation.

From this study, it can be seen that the Coffin-Manson fatigue life relationship is a reasonable model for estimating fatigue life of solder interconnects. The model constants derived from CLCC component testing provided reasonable agreement with test results form standard surface mount package types used in printed wiring board assemblies. Finally, the Engelmaier formulation for the strain range of leaded component package types results in non-conservative overestimation of cycles to failure. The leadless strain range model that does not square the temperature range is found to be a better match for all of the test data and package types examined in this paper.

**Acknowledgements**

The research for this paper was performed at Center for Advanced Life Cycle Engineering (CALCE) of University of Maryland under the sponsorship of Electronics Products and Systems Consortium. This Consortium is actively involved in studying the reliability of electronic interconnects under various environmental stress and loading conditions. The author would also like to thank Tom Woodrow (Boeing) for his encouragement and review of this paper.

References

1. Engelmaier, W., "Fatigue Life of Leadless Chip Carrier Solder Joints During Power Cycling," *IEEE Transactions on Components, Hybrids, and Manufacturing Technology*, Vol. 6, Issue: 3, September 1983, pp. 232 -237.
2. Dasgupta, A., C. Oyan, D. Barker and M. Pecht, M., "Solder Creep-Fatigue Analysis by Energy-Partitioning Approach," *Transactions of the ASME*, Vol. 114, June 1992, pp. 152-160.
3. Clech, J., J. Manock, D. Noctor, F., Bader, and J. Augis, "A Comprehensive Surface Mount Reliability Model (CSMR) Covering Several Generations of Packaging and Assembly Technology*,",Proceedings of the 40th Electronic Components and Technology Conference, 1993*, pp. 62- 70.
4. Darveaux, R., "Solder Joint Fatigue Life Model," *Proceedings of the TMS Annual Meeting*, Orlando, FL, 1997, pp. 213-218.
5. Syed, A., "Predicting Solder Joint Reliability for Thermal, Power, and Bend Cycling within 25% Accuracy," *Proceedings of the 51st Electronic Components and Technology Conference*, 2001, pp. 255-263.
6. Jih, E., and Y. Pao, "Evaluation of Design Parameters for Leadless Chip Resistors Solder Joints," *Transactions of the ASME, Journal of Electronic Packaging,* Vol. 117, Vol.117, June 1995, pp. 94-99.
7. Clech, J-P., "Solder Reliability Solutions: A PC-based Design-for-Reliability Tool," *Proceedings of the Surface Mount International Conference*, September 8-12, 1996, San Jose, CA, pp. 136-151.
8. IPC-SM-785, *Guidelines for Accelerated Reliability Testing of Surface Mount Solder Attachments*, IPC, Northbrook, IL, 1992.
9. IPC-9701, *Performance Test Methods and Qualification Requirements for Surface Mount Solder Attachments,* IPC, Northbrook, IL, 2002.
10. Osterman, M., A. Dasgupta, and B. Han, "A Strain Range Based Model for Life Assessment of Pb-free SAC Solder Interconnects," *Proceedings of the Electronic Components and Technology Conference*, 2006, pp. 884-890.
11. Hillman, D. and R. Wilcoxon, *JCAA/JG-PP No-Lead Solder Project:-55ºC to +125ºC Thermal Cycle Testing Final Report*, March 15, 2006.
12. Woodrow, T., "JCAA/JG-PP Lead Free Solder Project: -20°C to +80°C Thermal Cycle Test," *Proceedings of the SMTA International Conference, Rosemont, IL*, USA, September 24-26, 2006, pp 825-835.